JOURNAL OF MATERIALS SCIENCE 23 (1988) 2943–2950

Mechanical properties of zinc–aluminium alloys extruded in the liquid–solid state

H. LEHUY
Industrial Materials Research Institute, National Research Council Canada, 75 De Mortagne Boulevard, Boucherville (Quebec) Canada J4B 6Y4

Zinc–aluminium alloy bars and wires were successfully extruded in the liquid–solid state with a liquid fraction higher than 15%. Fully dense materials were obtained in this way with pressure lower than 100 MPa. The relationship between flow stress and solid fraction was obtained and the role of the liquid component in the deformation behaviour was clarified. Mechanical properties of the extruded material are presented and discussed with regard to the initial microstructure of the metals before deformation, i.e. the conventional dendritic structure and non-dendritic structure composed of solid spheroids dispersed in the remaining liquid obtained by stir-casting techniques. The microstructure of the extruded products was generally fine and a fibrous structure was easily observed particularly for the stir-cast material where primary solid spheroids were highly deformed. Optimization of these parameters leads to a desirable high-strength material.

1. Introduction

There are many recent reports in the literature describing studies on metal forming in the liquid–solid state at temperatures above the solidus. Some of the processes, such as rheocasting [1, 2], thixocasting [3, 4] or squeeze casting [5, 6] are recognized as belonging to the field of casting. These processes take advantage of the characteristics of alloys in their liquid–solid state, such as a remarkable decrease in flow stress and high formability [7, 9], while others are related to the malleability of the metals during forming. Liquid–solid metal extrusion is one of the latter processes taking advantage of the reduced extrusion forces. General aspects of mushy-state extrusion were studied by Kiuchi *et al.* [10] on materials of initially dendritic structure and their results showed a drop in the extrusion pressure to 20 to 25% of that for conventional hot extrusion as the solid fraction decreased from 100% to 70 to 80%. Looking into the flow behaviour of dendritic Sn–Pb slurries, Pinsky *et al.* [11] reported that the flow of semi-solid metals exhibits a visco-plastic strain-rate dependence. On the other hand, non-dendritic semi-solid Sn–Pb alloys prepared by a rheocasting technique were investigated by Taha and Suéry [12] using extrusion and the results showed an increased malleability of the non-dendritic material. However, no other work has been conducted and the properties of extruded materials have not been studied.

This work is a continuation of these investigations and is an effort to develop a better knowledge of the deformation of liquid–solid materials.

Dendritic and non-dendritic (spheroidized structure) materials of ZA-27 zinc–aluminium alloy were extruded after being reheated above the solidus. The structural changes of the liquid–solid slurries were followed and the conditions of stable extrusion were considered. In addition, the mechanical properties of the extruded materials were measured and compared to the properties of conventional casting and die-casting materials.

2. Experimental details

2.1. Materials characteristics

The base alloy in this study was a commercial zinc–aluminium alloy named ZA-27 developed for casting

TABLE I Characteristics of the Zn–Al alloy studied

Base Alloy		Specimen	Phases	Zn (wt %)	Al (wt %)	Cu (wt %)
Composition of ZA 27:	25 to 28Al; 2 to 2.5Cu; 0.15Mg bal. zinc (wt %)	Dendritic:				
		Dendrites	alpha	55	43	2
		Eutectic matrix	zinc + epsilon	93	3	4
Temperature (°C):		Stir-Cast:				
Liquidus	492	Primary	alpha	52	47	1
Eutectic	382	Secondary dendrites	beta	80	18	2
		Eutectic matrix	zinc + epsilon	92	4	4

0022–2461/88 $03.00 + .12

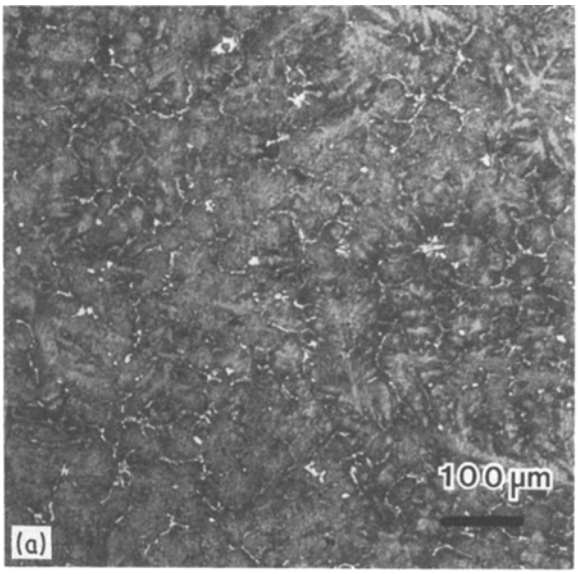

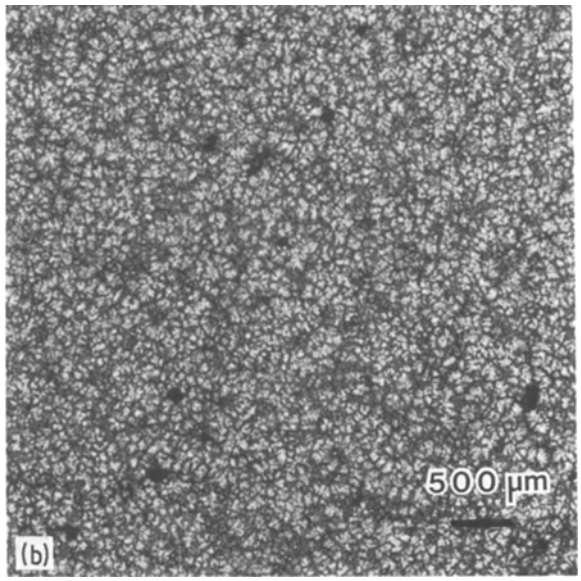

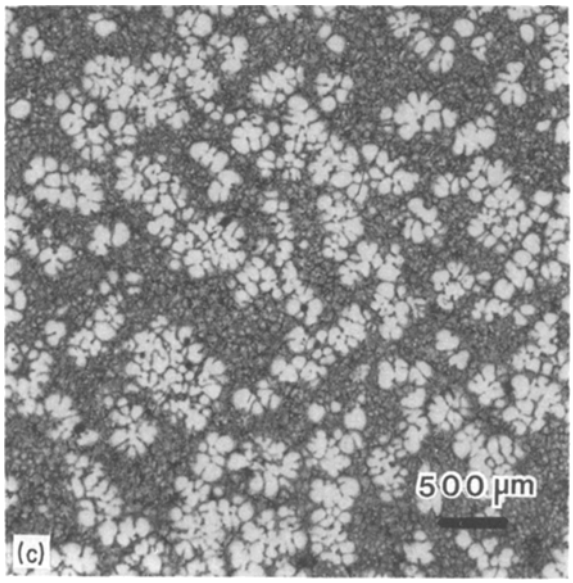

Figure 1 Microstructures of the studied materials: (a) coarse dendrites, (b) fine dendrites, (c) stir-cast.

applications. The nominal composition of the alloy, its solidification characteristics and phases are given in Table I. Three types of structure were selected for this investigation: two conventionally cast materials with, respectively, coarse and fine dendritic structures and a stir-cast material with a structure composed of spheroidized solid particles embedded in a residual liquid. The coarse dendritic material was prepared by casting melts in a preheated graphite mould with a superheat of 50° C, by which procedure results a dendritic equiaxed microstructure throughout the ingot as shown in Fig. 1a. The average secondary dendrite arm spacing ranged from 100 to 200 μm. The fine dendritic material was prepared by casting in a cold graphite mould at 490° C, i.e. 2° C below the liquidus temperature. In this way, a fine dendritic structure with primary dendrite arm spacing of less than 50 μm and secondary dendrite arm spacing of less than 20 μm was obtained, as shown in Fig. 1b. However, as it was cast below the liquidus, some primary solid particles, occupying less than 3 vol % of the material, were dispersed throughout the ingot. On the other hand, stir-cast materials were prepared by mechanical stirring of the alloy during solidification. Details of the stir-casting technique used for the preparation of the ingots and the characteristics of stir-cast slurries have been published [13]. At 470° C, stir-cast materials exhibit 30 vol % primary particles as shown in Fig. 1c. These latter are fairly round in shape and are homogeneously distributed throughout the ingots; the interparticle material displays a rapid solidification structure. The structural dimensions of the studied materials are given in Table II. The cast ingots were subsequently machined into cylindrical samples, 3.90 cm (1.5 in.) diameter and 10 cm (4 in.) high, for extrusion experiments.

The ingots were partially remelted in the range 382 to 445° C prior to extrusion. The characteristics of ZA-27 alloy in the liquid–solid state near the solidus (437° C) are complex because of the presence of a multiphase microstructure as shown in the phase diagram in Fig. 2. Above 382° C, the eutectic occupying approximately 10 vol % is remelted. Between the eutectic temperature and the solidus, 437° C, the β phase is partially remelted and the liquid fraction

TABLE II Microstructure of studied materials

Casting conditions	Type	Dimensions (μm)
50° C Superheat castings	100% coarse dendrites	100–200
490° C Castings	97% fine dendrites	< 25
	3% primaries	< 100
Stir-cast 470° C	70% fine dendrites	< 25
	30% primaries	100–500

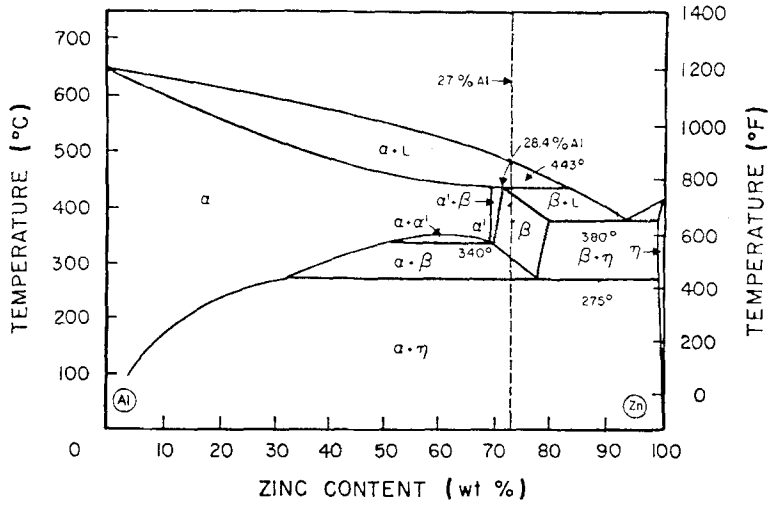

Figure 2 Phase diagram of the binary Zn–Al system.

reaches approximately 15%. Above this temperature, the remelting rate increases rapidly and at 445° C the remelted liquid amount is near 40%, as shown in Fig. 3 where the solid fraction is plotted against the temperature. From this figure, the following empirical equation can be deduced by curve fitting

$$f_s = 18072 - 134.6T + 0.336T^2 \quad (1)$$

where f_s is the solid fraction (%) and T the temperature in the range 382 to 460° C.

2.2. Extrusion procedure

Fig. 4 shows a schematic diagram of the experimental device capable of extruding billets of up to 5 cm diameter. The device was set up on a vertical type 250 kN servo-hydraulic testing machine controlled by a computer. The die, punch and container were heated simultaneously to the required temperature by electrical elements at which point the billet was placed in the container. The temperature was measured with thermocouples inserted into the die, container and billet. Extrusion tests were performed at constant velocity with measurements of the plunger displacement and extrusion force.

In order to follow the different mechanisms which govern the metal flow, various types of dies such as shear (or flat-faced), parabolic and streamlined [14] were used. With a shear die, the material was extruded principally through shear deformations, while with converging dies, the material flowed through a combination of hydrostatic and shear deformations. The objective of this application is to improve the workability of the billets: press load, extrusion speed and quality of the products.

Extruded products were subjected to uni-axial tensile and Charpy tests using standard methods put forward by the ASTM for light alloys [15]. Finally the mechanical results were related to the microstructural observations.

3. The liquid–solid metal extrusion behaviour

Typical behaviour of the material during extrusion is shown in Fig. 5 where the extrusion pressure, defined as the extrusion force acting on a unit area of plunger

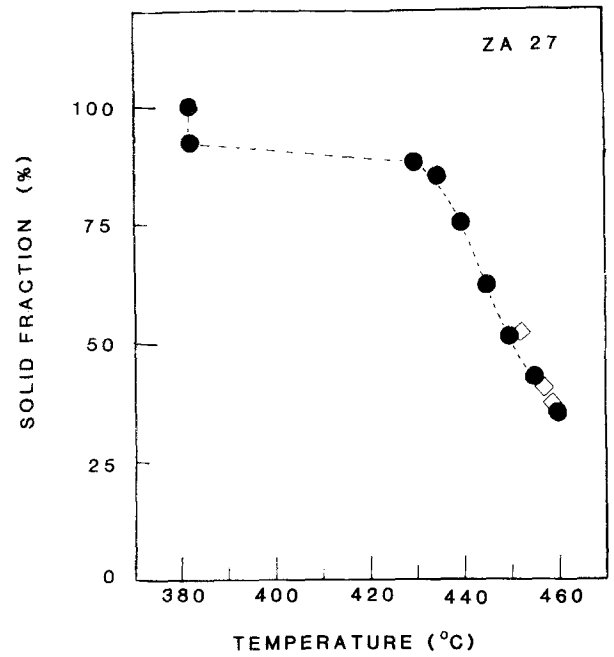

Figure 3 Solid fraction of stir-cast ZA-27 plotted against the remelt temperature, from (●) LeHuy [13], (◇) Murphy [20].

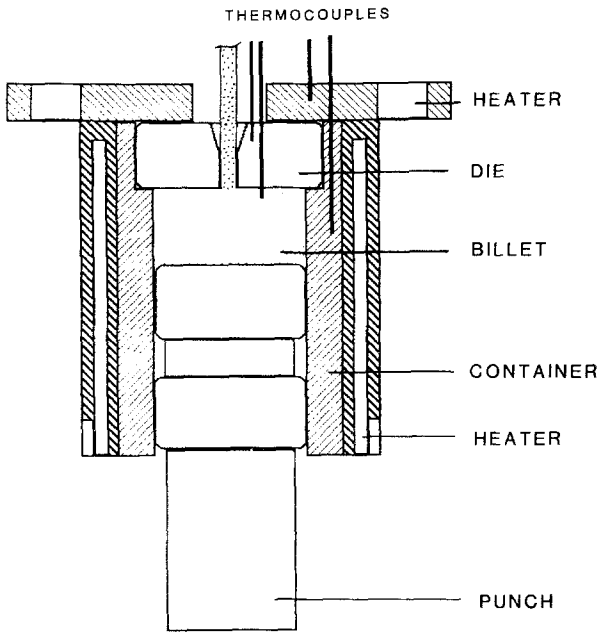

Figure 4 Schematic diagram of extrusion apparatus showing container, punch, die and billet.

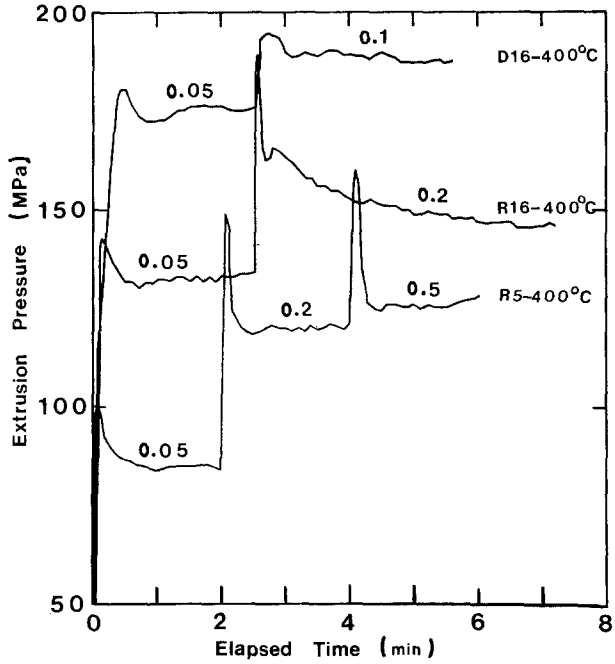

Figure 5 Extrusion pressure–time curves: R5-400, stir-cast material, reduction ratio 5, temperature 400° C; R16-400, stir-cast material, reduction ratio 16, temperature 400° C; D16-400, dendritic materials, reduction ratio 16, temperature 400° C. Ram speed in mm sec^{-1}; shear die.

cross-section, is depicted as-measured during the deformation. In these experiments, a shear (or flat-faced) die was used and the extrusion temperature was maintained constant at 400° C, i.e. with less than 15% of liquid fraction. The extrusion curves of stir-cast material submitted to reduction ratios of $R = 5$ and $R = 16$ and of dendritic material submitted to a reduction ratio of $R = 16$ are shown, respectively, as R5-400, R16-400 and D16-400, in the figure. In every case, the curves exhibit the same features. With regard to the R5-400 curve, the extrusion pressure passes through a maximum, after which the stress decreases a little, then holds constant. When the ram speed is increased to a higher value, i.e. passing from 0.05 to 0.2 mm sec^{-1}, the stress passes through another maximum before it reaches a new constant level. The constant stress at which homogeneous flow occurs is called the steady-state extrusion pressure. Pinsky *et al.* [11] have already described this phenomenon and have associated it with a "compaction" mode, whereby excess liquid metal is squeezed out of the matrix, followed by a "flow mode". Nevertheless, our tests indicate that the "compaction" mode is influenced more by the stiffness of the materials than by the amount of dripping liquid metal, because no extra liquid metal was squeezed out during the change of the ram velocity although a pressure peak was observed. Otherwise, the height of the pressure peak tended to decrease with increase of the remelting liquid.

3.1. Extrusion pressure versus ram speed

Extrusion data corresponding to steady-state measurements are grouped in Fig. 6 where extrusion pressure is plotted against the ram speed for both dendritic and stir-cast materials at different temperatures and reduction ratios. For this series of tests, the shear die was used to enhance the shearing effects of the deformation. Data show that dendritic materials need higher temperature or higher pressure to deform than spheroidized ones. This is consistent with experimental observations reported in earlier work [12].

During extrusion of fully solid metal, the extrusion pressure can be expressed as a function of the reduction ratio as follows [16]

$$\sigma = (A + B \ln R)\sigma_0 \qquad (2)$$

with R the reduction ratio, σ_0 the flow stress and A and B constants.

From Equation 2, Taha and Suéry [12] derived a relation applicable for liquid–solid metal by combining this with the pseudo-plastic strain-rate dependence of the flow stress

$$\sigma = K(A + B \ln R) \exp(bf_s)\dot{\gamma}^n \qquad (3)$$

with $\dot{\gamma}$ the strain rate and K and b constants.

Equation 3 expresses the pseudoplasticity of the slurries through the strain rate $\dot{\gamma}$. Using data from Fig. 6, values of the strain-rate sensitivity, n, calculated for ZA-27 slurries range from 0.1 to 0.2 and

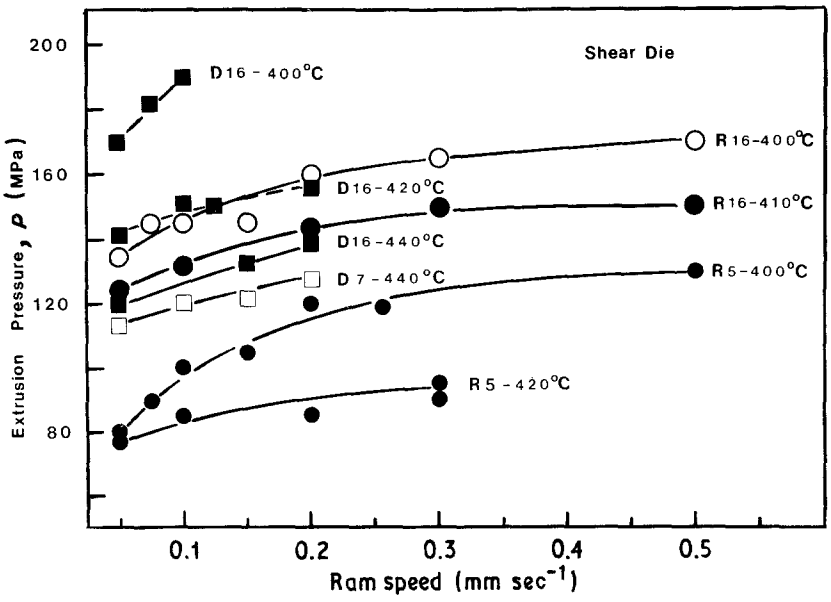

Figure 6 Relationship of extrusion pressure to ram speed. (○, ●) Stir-cast, (□, ■) dendritic.

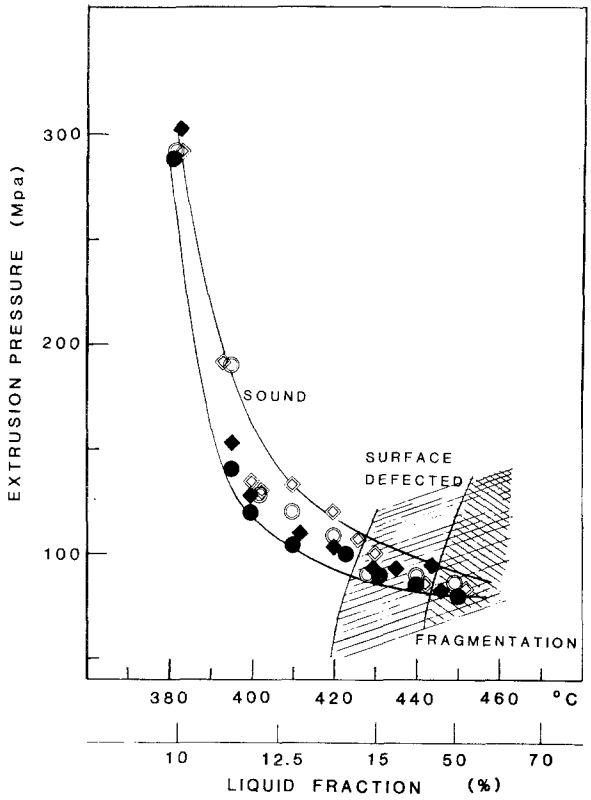

Figure 7 Extrusion pressure plotted against extrusion temperature: (● ◆) streamlined die; (○ ◇) parabolic die, reduction ratio 16, ram speed 0.5 mm sec^{-1}. (●, ○) Stir-cast, (◆, ◇) dendritic.

are of the same order of magnitude as those reported for other alloys [11]. On the other hand, the high dependence of extrusion pressure on the slurry temperature is expressed by the exponential term of the volume fraction of the solid phase. This relationship could be followed in isothermal studies with all other variables constant.

3.2. Extrusion pressure versus extrusion temperature

For this series of tests, the reduction ratio and the ram speed were kept constant at $R = 16$ and $v = 0.5$ mm sec^{-1}, respectively. Fig. 7 shows results of steady state pressure plotted against extrusion temperature for both dendritic and stir-cast materials and for both parabolic and streamlined dies. For high volume fraction of solid phase, the extrusion pressure was higher for the dendritic materials than for the non-dendritic ones, but at higher extrusion temperature, the behaviour became quite similar for both structures. Increasing the extrusion temperature from 382° C (i.e. eutectic temperature) to 420° C, the extrusion pressure decreased markedly, passing from 300 MPa to 120 MPa, the extrusion pressure decreased markedly, passing from 300 MPa to 120 MPa. Above 420° C, the slope of the pressure curve flattens and radial cracks appeared on the surface of the rods. Unstable extrusion occurred above 440° C leading to fragmentation of the extruded rods. Examination of the fracture revealed an intergranular type, due probably to the low strength of the material at the die exit and to the amount of remelted metal.

Compared with theory as defined by Equation 3, the experimental data vary less markedly with the volume fraction than the calculations predict. The reasons for this discrepancy are numerous. To explain the disagreement Taha and Suéry [12] suggested a different influence of f_s on the viscosity and on friction between the material and the die. Our observations indicate that when the temperature increases, the resulting increased volume of liquid phase tends to flow independently towards the die exit during the "compact" mode, thereby diminishing the amount of liquid phase in the slurry when the stable extrusion mode is reached. During the "flow mode", the actual solid fraction was changed and was not the fraction that would be expected from the temperature. Moreover, softening of the solid fraction with increasing temperature is not included in the formulation of Equation 3. Work is currently in progress to shed more light on these phenomena in order to take account of an effective solid fraction.

The distinction between stable and unstable extrusion is also shown in Fig. 7. Below 425° C (i.e. 15% f_s), the extruded products were sound even at a high extrusion speed of 1 mm sec^{-1}. Above this temperature, radial cracks appeared on the surface of the rods, whereas at 442° C and higher, the extruded rods were fragmented. At this temperature, the extrusion must be carried out at sufficiently low ram speed to avoid hot shortness; for example sound products could be obtained at a temperature as high as 445° C ($\sim 40\%$ f_s) but only with a maximum ram speed of 0.1 mm sec^{-1}.

3.3. Converging die versus shear die

The use of converging dies such as the parabolic or streamlined type instead of a shear die markedly improves the quality of the product. With a shear die, the extrusion pressure was higher by about 30% than with converging dies, but the most important factor with a shear die is the difficulty to increase the ram speed above 0.2 to 0.3 mm sec^{-1}, without the appearance of radial cracks on the rods. Modelling of the shear die shows considerable temperature increase at local points within the shearing material. On the other hand, the converging dies have smooth entry, avoiding sharp velocity discontinuities through the deformation area. Experience has shown that both types, parabolic (square spline fits) and streamlined (cubic spline fits), produced equivalent results particularly at high temperature as shown in Fig. 7. The quantitative features of these tests and their numerical modelling will be published elsewhere [17].

4. Mechanical properties

4.1. Tensile test

Fig. 8 shows the tensile strength of extruded materials plotted against the extrusion temperature. The tensile strength was in the range 425 to 480 MPa depending on temperature and microstructure with an elongation at fracture not less than 5%. Products obtained from fine dendritic base materials show the best properties with a tensile strength varying from 450 to 475 MPa. The reproducibility of the results is good; however, a slight variation of tensile strength was observed along an extruded bar as indicated by results numbered 1 to

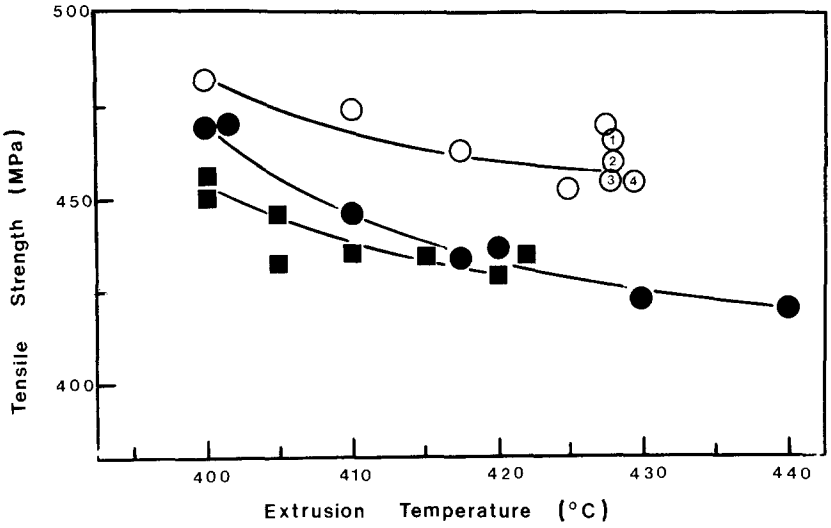

Figure 8 Effects of extrusion temperature on tensile strength of ZA-27 extruded materials (numbers 1 to 4 represent specimens at various places along the same bar). Dendrites: (○) fine, (●) coarse, (■) Stir-cast, 470° C.

4 on the figure which were obtained from specimens taken at several points from the beginning to the end of the bar. For comparison, data found in the literature on other forming processes [18] indicated ZA-27 tensile strength ranging between 350 and 440 MPa.

Heat treatment of the materials in the solid–liquid state prior to extrusion modifies their structure. Fig. 9 shows the structure transformation of a stir-cast material before and after it was heated to 430° C. The primary particles vary slightly whereas the secondary dendrites are fully spheroidized. During the extrusion, the primary particles, appearing black on this electron micrograph, were severely deformed and a fibrous structure was obtained (see Fig. 10a). During the air-cooling stage after deformation, both the fibres and the matrix recrystallized as can best be seen on the enlarged micrograph shown in Fig. 10b. Similarly, the epsilon phase, rich in zinc and copper, which is embedded in the liquid ternary eutectic, is severely deformed and fragmented under deformation. During the air-cooling stage after extrusion, the epsilon fragments grow throughout the liquid (Figs 11a and b), drawing elements from it, as can be seen by the excrescences along particle boundaries. The fragmentation of the intermetallic particles can partially explain the high strength of these materials.

4.2. Effect of temperature on tensile strength and elongation

Fig. 12 shows the dependence of tensile strength and elongation of extruded ZA-27 on the temperature. The three initial types of structure are also illustrated. By increasing the testing temperature from room temperature to 100° C, the tensile strength drops by 35% from 450 to 300 MPa, whereas the elongation increases from 10% to 22%. This high dependency on temperature seems important; however, it is of the same order as that found in other investigations. Tensile properties of gravity-cast ZA-27 published by ILZRO [19], represented by dotted lines in the same figure, indicate a drop from 415 MPa at room temperature to 300 MPa at 80° C. Stir-cast materials, tested by Mykura and Murphy [20], have an as-cast tensile strength of approximately 375 MPa which decreases to 250 MPa at 100° C; the full Murphy's strength against temperature curve is shown as a dashed line in Fig. 12.

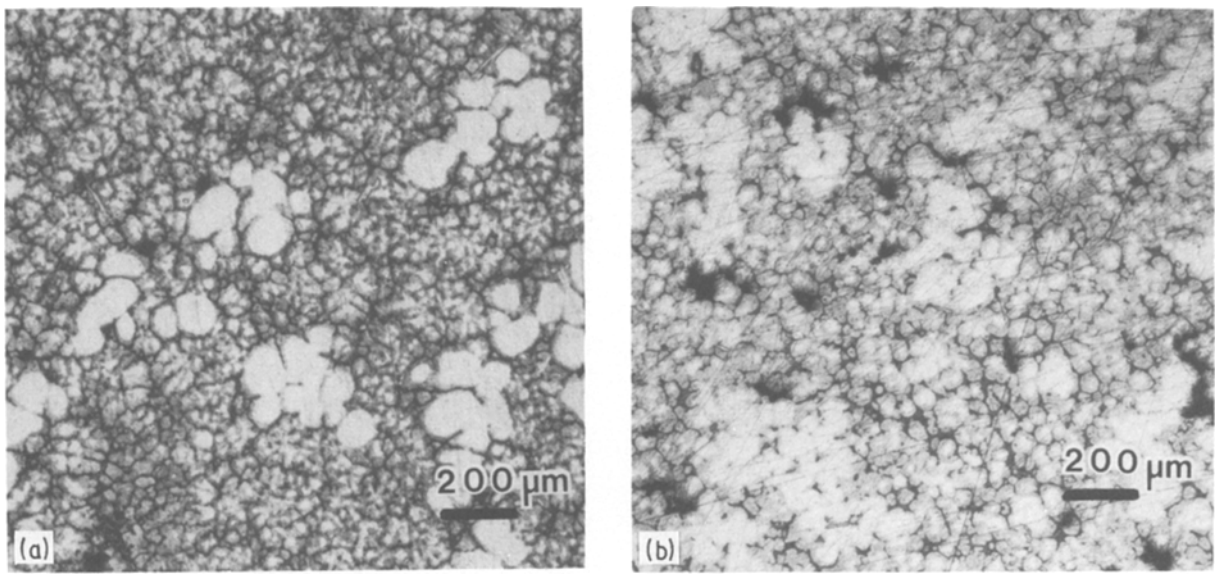

Figure 9 Effect of heat treatment on microstructure of stir-cast materials: (a) as stir-cast; (b) after heat treatment at 430° C.

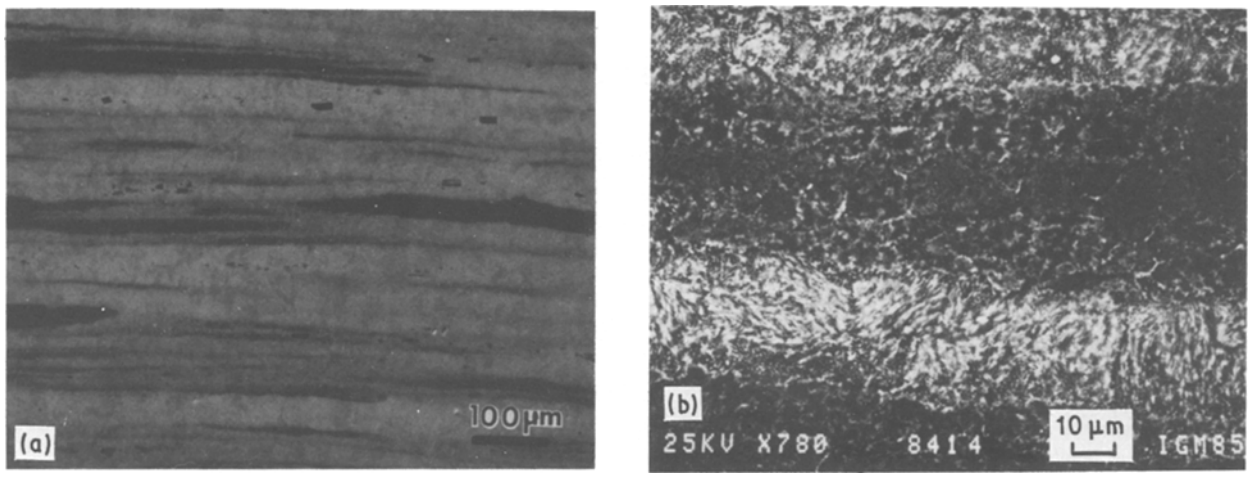

Figure 10 Microstructures of extruded material: (a) deformation of primary particles; (b) enlarged micrograph showing the recrystallized structure.

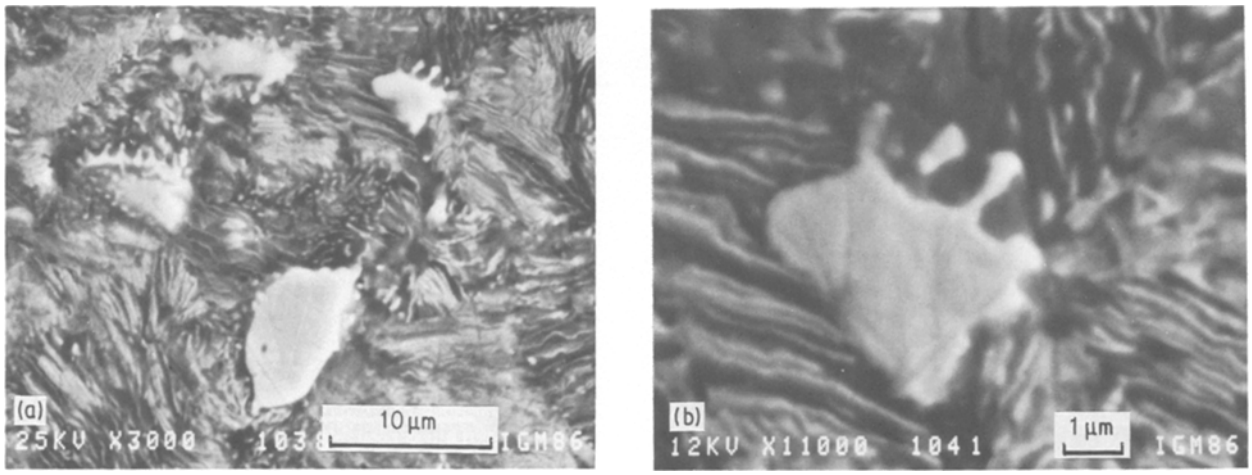

Figure 11 Fragmentation of epsilon phase: excrescence of secondary solidification can be seen in (b).

4.3. Charpy tests

Charpy tests were performed at room temperature on 10 mm × 10 mm unnotched specimens, and Table III summarizes the results. For as-stir-cast materials, the impact strength is low, generally under 10 J. This was principally attributed to the porosity present in the materials. When highly densified by the HIP process (i.e. 350° C, 2 h with 180 MPa of pressure), the results were 45 to 65 J, comparable with the properties of conventional cast materials found in the literature [18].

Extrusion increases the impact strength to as high as 130 to 140 J for stir-cast base materials. The superiority of stir-cast materials over the dendritic ones is due to the increase of ductility as can be observed from the Charpy test results. Effectively the maximum impact load is practically the same on the two specimens. Examination of the fracture surface shows that extensive stretching before fracture, with dimples originating from aluminium-rich phases, explains the high impact strength of these materials.

TABLE III Impact strength 10 mm × 10 mm bar unnotched of various ZA-27 materials

	Energy (J)
As stir-cast	< 10
Stir-cast + HIP	45–65
Dendritic + extrusion	85–95
Stir-cast + extrusion	130–140

5. Conclusions

Metal forming of dendritic and non-dendritic ZA-27 alloy in the liquid–solid state was investigated by extrusion. Results show that:

1. Bars and wires were extruded successfully with small force and high reduction ratio.

2. Extrusion of liquid–solid alloy is composed of two sequential stages: (a) compaction of the solid matrix with squeezing out of excess liquid metal, (b) stable extrusion of the solid matrix with the remaining liquid.

3. Stable extrusion of liquid-solid alloy obeys the power-law,

$$\sigma \propto \exp(bf_s)\dot{\gamma}^n$$

4. An effective solid fraction, f_s, is needed to take account of liquid losses.

5. For high volume of solid phase (> 85%), the extrusion pressure is higher for dendritic materials than for stir-cast ones.

6. For low volume of solid phase (85% > f_s > 50%), the behaviour is quite similar for both structures.

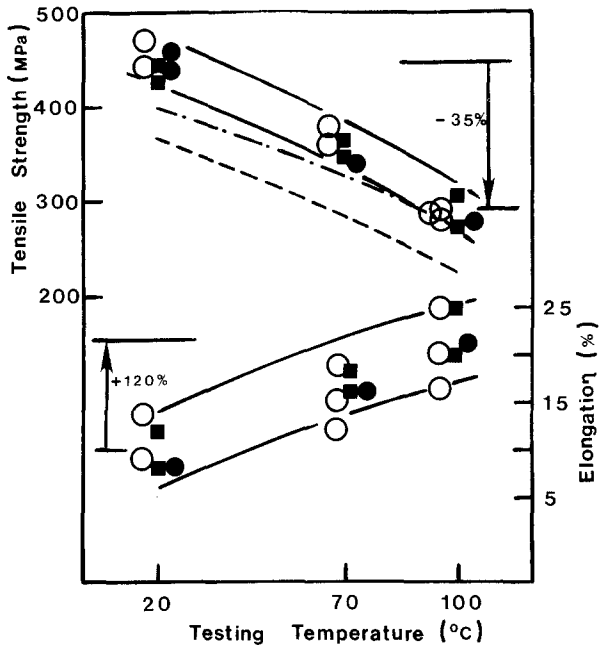

Figure 12 Effects of testing temperature on tensile strength and elongation of extruded ZA-27 materials. Literature data are shown for comparison: (—·—) conventional casting [19]; (– – –) stir casting [20]. Dendritic: (●) coarse, (○) fine. (■) Stir-cast, 470° C.

7. The products are sound when the solid fraction is over 85%.

8. At higher temperature, radial cracks could be avoided by lowering the extrusion speed.

9. Dendritic materials are finely recrystallized with a grain size under 10 μm.

10. The extruded stir-cast materials exhibit a textured structure with ductile aluminium-rich fibres.

11. Extruded materials show excellent mechanical properties that equal or exceed the best accepted values published to date for conventional forming processes.

Acknowledgements

The author thanks R. Lavallée for his technical assistance and Dr D. C. Briggs of CANMET and J. Blain for their invaluable advice.

References

1. "Rheocasting", in Proceedings of a workshop held at the AMMRC (1977), MCIC Report, Columbus, Ohio.
2. J. COLLOT, Mem. et Études Scientifiques, *Revue de Métallurgie* **81** (21) (1984) 591.
3. M. C. FLEMINGS and R. MEHRABIAN, Proceedings of the 40th International Foundry Congress (1973) Moscow, No. 9, p. 1.
4. F. C. BENNETT, T. E. LEONTIS and S. L. COULING, Proceedings of the 34th Annual Meeting of the International Magnesium Association (International Magnesium Association, Bayton, Ohio, 1977) p. 23.
5. S. RAJAGOPAL, *J. Appl. Metalworking* **1** (1981) 3.
6. G. WILLIAMS and K. M. FISHER, *Metals Technol.* (1981) 263.
7. P. A. JOLY and R. MEHRABIAN, *J. Mater. Sci.* **11** (1986) 1393.
8. V. LAXMANAN and M. C. FLEMINGS, *Met. Trans. A* **13A** (1982) 1809.
9. H. LEHUY, J. BLAIN and J. MASOUNAVE, Proceedings of the Zinc Aluminum Symposium, 25th Annual Conference of Metallurgists, CIM, 1986, Toronto, p. 143.
10. M. KIUCHI, S. SUGIYAMA and R. ARAI, 2nd Report, Proceedings of the 20th International MTDR Conference, 1979, Birmingham, p. 79.
11. D. A. PINSKY, P. O. CHARREYRON and M. C. FLEMINGS, *Met. Trans. B* **15B** (1984) 173.
12. M. A. TAHA and M. SUÉRY, *Metals Technol.* **11** (1984) 226.
13. H. LEHUY, J. MASOUNAVE and J. BLAIN, *J. Mater. Sci.* **20** (1985) 105.
14. J. S. GUNASEKERA, H. L. GEGEL, J. C. MALAS, S. M. DORAIVELU and D. BARKER, *J. Appl. Metalworking* **4** (1985) 43.
15. ASTM Standard B557-84 in 1986 Annual Book of ASTM Standards, Vol. 03.01 (American Society for Testing and Materials, Philadelphia, Pennsylvania, 1986) p. 58.
16. P. AVENAS, "Mise en forme des métaux et alliages", Edition of CNRS, (1976) p. 185.
17. H. LEHUY, *Mech. Mater.* to be published.
18. E. GERVAIS, R. J. BARNHURST and C. A. LOONG, *J. Metals* **11** (1985) 43.
19. "Engineering Properties of Zinc Alloys", 2nd Edn (International Lead Zinc Research Organization, New York, 1981).
20. M. MYKURA and S. MURPHY, Proceedings of the Zinc Aluminium Symposium, 25th Annual Conference of Metallurgists, CIM, 1986, Toronto, p. 45.

Received 8 September
and accepted 10 December 1987